# Accurately Capturing Global Tides in a Loosely-Coupled Ocean Circulation and Global Storm Tide Model

Coleman P. Blakely [1] William Pringle [2] Damrongsak Wirasaet [1]
Joannes J. Westerink[1]

[1]University of Notre Dame, Notre Dame, IN, USA

[2]Environmental Science Division, Argonne National Laboratory, Lemont, IL, USA

3rd International Workshop on Waves, Storm Surges, and Coastal Hazards; 17th International Workshop on Wave Hindcasting and Forecasting
October 5, 2023

# Overview

# Overview

# Motivation

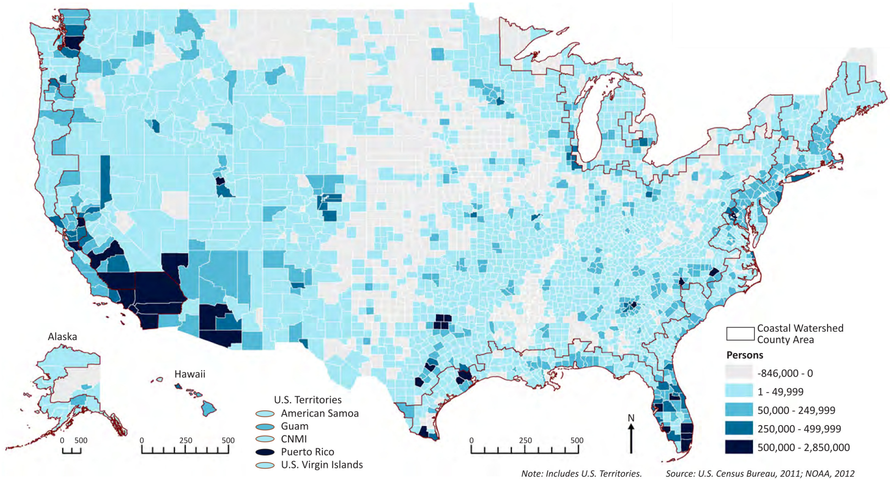


Figure: Change in population in US counties 1970-2010 (Image courtesy of NOAA) [10]

# Motivation

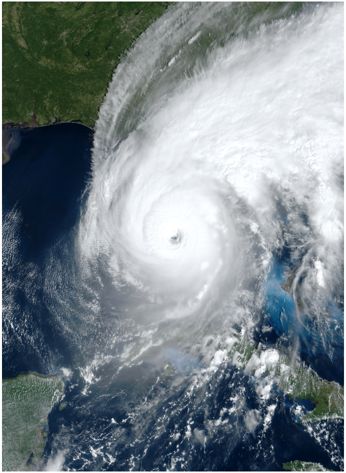

Figure: Image courtesy of NOAA GOES

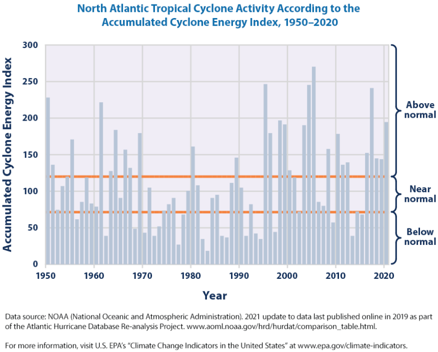


Figure: Figure courtesy of US EPA

# Motivation

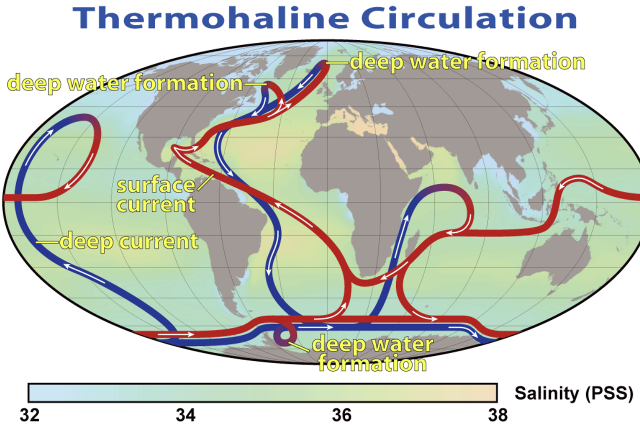


Figure: Image courtesy of NASA

# Background

- Storm Tide modeling historically performed with high resolution, depth-averaged regional models [2, 8, 12]

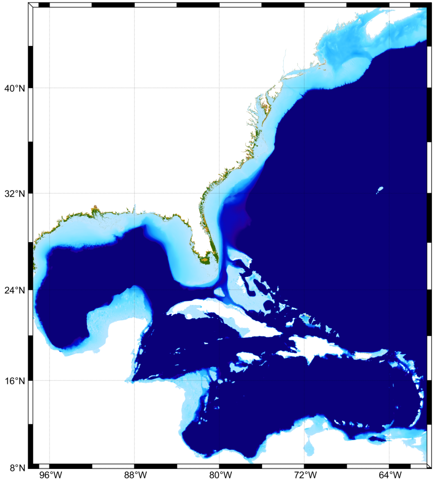

# Background

- Storm Tide modeling historically performed with high resolution, depth-averaged regional models [2, 8, 12]
- Ocean modeling historically performed with coarser, depth resolving, global models[1][9, 1]

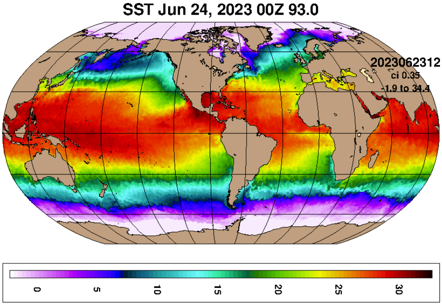


[1]Image courtesy of GOFS3.1 website [4]

# Background

- Storm Tide modeling historically performed with high resolution, depth-averaged regional models [2, 8, 12]
- Ocean modeling historically performed with coarser, depth resolving, global models[1] [9, 1]
- Recent developments have allowed for high resolution 2D global models [11, 13]

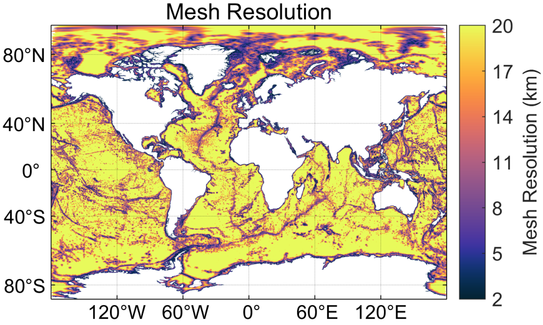


[1] Image courtesy of GOFS3.1 website [4]

# Background

## Problem

How do we bridge the gap in scales to capture deep-ocean, density driven, baroclinic effects present in Ocean Global Circulation Models (OGCMs) while maintaining the quality of results seen in high-resolution, barotropic, total water level models?

# Research Scope

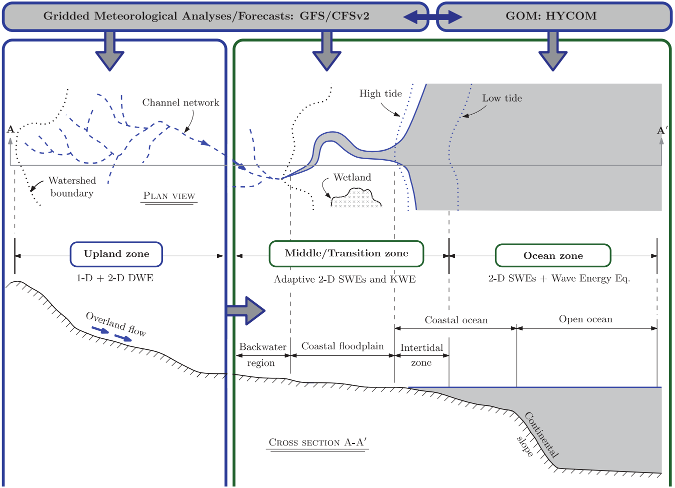


Figure: Proposed coupling framework

# Research Scope

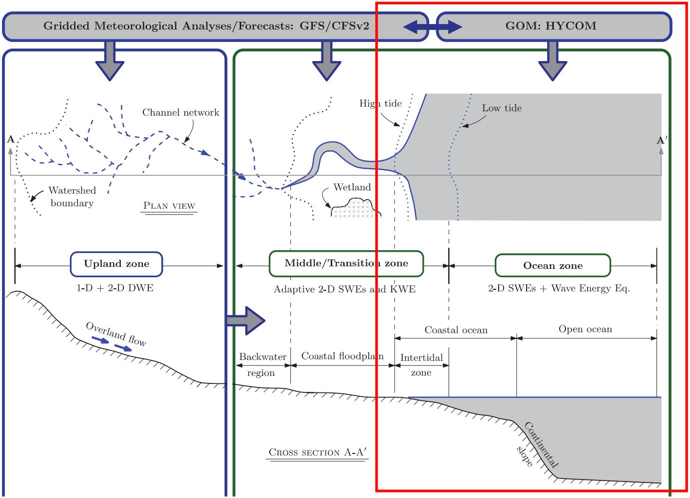

# ADCIRC2D$^+$ Coupling Framework

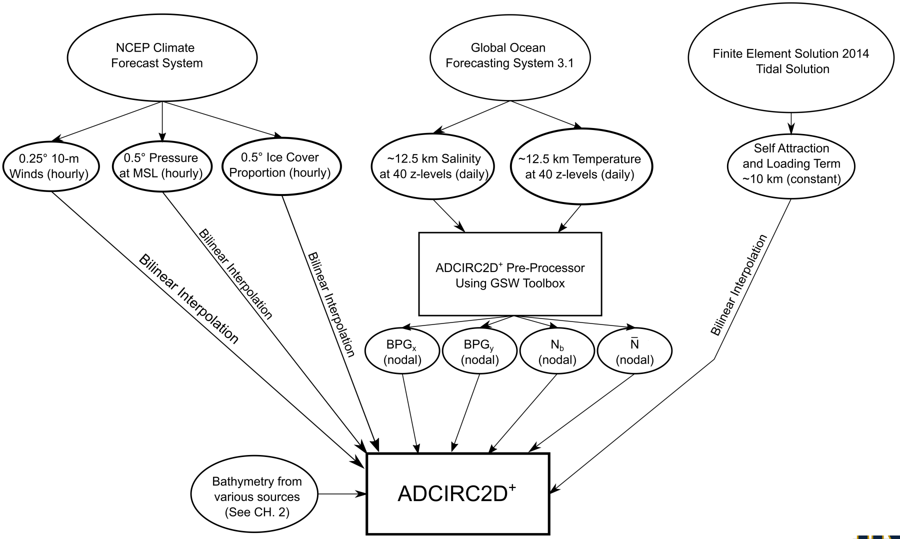

# Overview

# Research Goals

## Research Goal

Deepen the understanding of how oceanic processes and their parameterizations within numerical models affects global total water levels. Develop approaches to incorporating these processes across scales in a physically consistent way to ensure accurate total water level predictions for use in a global forecasting model.

# Research Goals

## Research Goal

Deepen the understanding of how oceanic processes and their parameterizations within numerical models affects global total water levels. Develop approaches to incorporating these processes across scales in a physically consistent way to ensure accurate total water level predictions for use in a global forecasting model.

## How?

Investigate methods to incorporate density-driven effects in a depth-averaged global total water level model while maintaining the accuracy of tidal results. Understand the physical reasons that modifications to the depth-averaged shallow water equations must be implemented and the best methods to implement them. Examine how externally derived density-driven effects impact total water levels in a hydrodynamic model.

# Governing Equations: Shallow Water Equations

$$\frac{\partial \eta}{\partial t} + \nabla \cdot (\boldsymbol{U} H) = 0$$

$$\frac{\partial \boldsymbol{U}}{\partial t} + \boldsymbol{U} \cdot \nabla \boldsymbol{U} + f \boldsymbol{k} \times \boldsymbol{U} = -\nabla \left[ \frac{\rho_s}{\rho_0} + g(\eta - \eta_{EQ} - \eta_{sal}) \right] + \frac{\boldsymbol{M}}{H} - \frac{\boldsymbol{D}}{H} - \frac{\text{BPG}}{H} + \frac{\tau_s}{\rho H} - \frac{\tau_b}{\rho_0 H} - \mathbb{C}$$

# Governing Equations: Shallow Water Equations

$$\frac{\partial \eta}{\partial t} + \nabla \cdot (\boldsymbol{U} H) = 0$$

$$\frac{\partial \boldsymbol{U}}{\partial t} + \boldsymbol{U} \cdot \nabla \boldsymbol{U} + f \boldsymbol{k} \times \boldsymbol{U} = -\nabla \left[ \frac{\rho_s}{\rho_0} + g(\eta - \eta_{EQ} - \eta_{sal}) \right] + \frac{\boldsymbol{M}}{H} - \frac{\boldsymbol{D}}{H} - \frac{\mathrm{BPG}}{H} + \frac{\tau_s}{\rho H} - \frac{\tau_b}{\rho_0 H} - \mathbb{C}$$

# Depth-Averaged Baroclinic Pressure Gradient

$$\text{BPG} = \int_{-h}^{\eta} \left( g\nabla \left[ \int_{z}^{\eta} \frac{\rho - \rho_0}{\rho_0} dz \right] \right) dz$$

Where,

$$\begin{aligned} h &= \text{Bathymetric depth below geoid} \\ \eta &= \text{Water height wrt geoid} \\ \rho &= \text{Density at depth z} \\ &= F(\text{temperature}, \text{salinity}) \\ \rho_0 &= \text{Reference Density} \end{aligned}$$

# Internal Tide Generation/Dissipation

$$\mathbb{C} = C_{it} \frac{\sqrt{\left(N_b^2 - \omega^2\right)\left(\bar{N}^2 - \omega^2\right)}}{4\pi\omega} \nabla h \boldsymbol{U_T} \nabla h$$

Where,

$$\begin{aligned} \boldsymbol{U_T} &= \text{Tidal component of velocity} \\ N_b &= \text{ Brunt-Väisälä frequency at seabed} \\ &= F(\text{temperature, salinity}) \\ \bar{N} &= \text{ depth averaged Brunt-Väisälä frequency} \\ &= F(\text{temperature, salinity}) \end{aligned}$$

# "Tidal" Velocities

## Question:

How do we isolate the "tidal" velocity and is it even necessary?

## Approaches:

1. Assume $\boldsymbol{U} \approx \boldsymbol{U_T}$

# "Tidal" Velocities

**Question:**

How do we isolate the "tidal" velocity and is it even necessary?

**Approaches:**

1. Assume $\boldsymbol{U} \approx \boldsymbol{U_T}$
2. Use a 25-hour lagged average filter to remove the tidal component of velocity and then let $\boldsymbol{U_T} = \boldsymbol{U} - \overline{\boldsymbol{U}}$

# "Tidal" Velocities

**Question:**

How do we isolate the "tidal" velocity and is it even necessary?

**Approaches:**

1. Assume $\boldsymbol{U} \approx \boldsymbol{U_T}$
2. Use a 25-hour lagged average filter to remove the tidal component of velocity and then let $\boldsymbol{U_T} = \boldsymbol{U} - \overline{\boldsymbol{U}}$
3. Use a high-pass filter that removes subtidal energy and let this filtered velocity be the tidal velocity.

# Filtering

$$y_{out} = \sum_{k=-n}^{n} \alpha_k y_k$$

## Approaches

- Approach 1 is essentially $n = 0$ with $\alpha_0 = 1$ (no filter whatsoever)

# Filtering

$$y_{out} = \sum_{k=-n}^{n} \alpha_k y_k$$

## Approaches

- Approach 1 is essentially $n = 0$ with $\alpha_0 = 1$ (no filter whatsoever)
- Approach 2 (hereafter LA25) filters out high-frequency (i.e., tidal) velocities with a low-pass filter where $n = 12$ and $\alpha_k = \frac{1}{25}$.

# Filtering

$$y_{out} = \sum_{k=-n}^{n} \alpha_k y_k$$

## Approaches

- Approach 1 is essentially $n = 0$ with $\alpha_0 = 1$ (no filter whatsoever)
- Approach 2 (hereafter LA25) filters out high-frequency (i.e., tidal) velocities with a low-pass filter where $n = 12$ and $\alpha_k = \frac{1}{25}$.
- Approach 3 (hereafter MHP) uses a high-pass filter with a filter length of 49 hours. This filter is derived from the low pass Munk "Tide Killer" Filter [7].

# Filtering

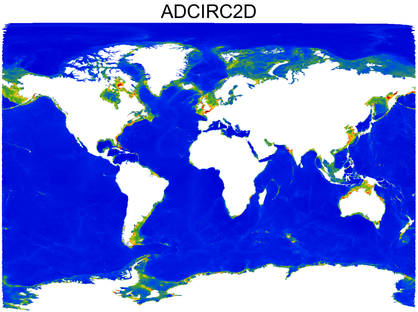


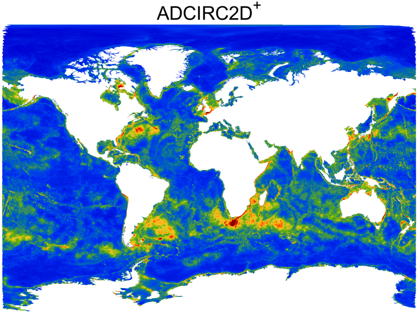

# Filtering

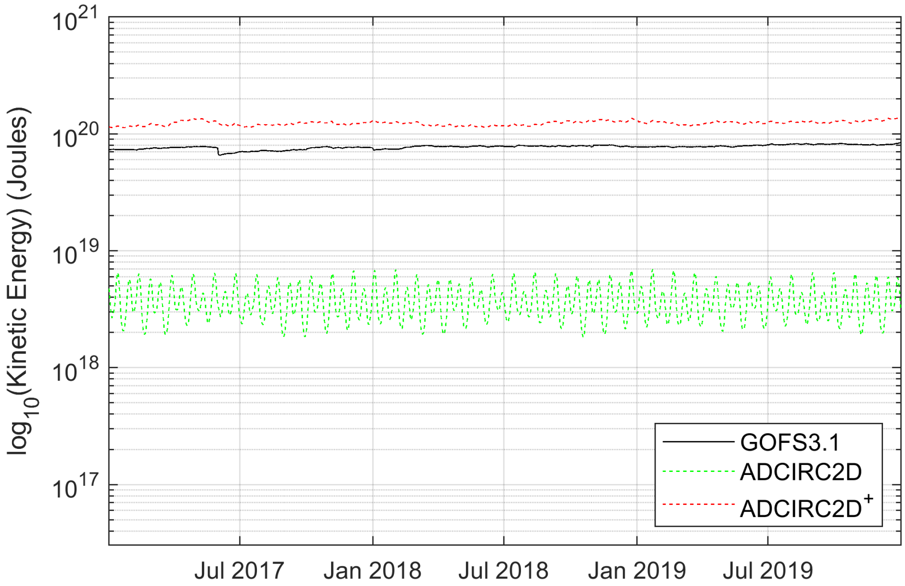

$10^{21}$
$10^{20}$
$10^{19}$
$10^{18}$
$10^{17}$
$\log_{10}$(Kinetic Energy) (Joules)
Jul 2017
Jan 2018
Jul 2018
Jan 2019
Jul 2019
GOFS3.1
ADCIRC2D
ADCIRC2D+

# Filtering

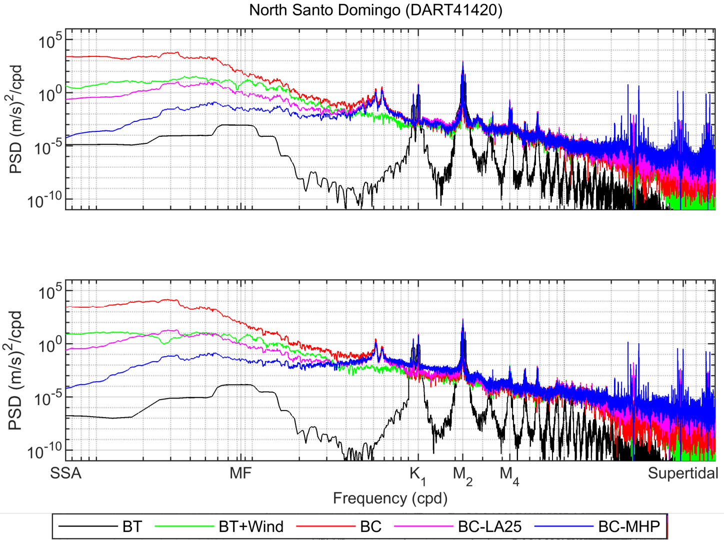

North Santo Domingo (DART41420)
$10^5$
$10^0$
$10^{-5}$
$10^{-10}$
PSD (m/s)$^2$/cpd
SSA
MF
$K_1$
$M_2$
$M_4$
Supertidal
Frequency (cpd)
BT
BT+Wind
BC
BC-LA25
BC-MHP

# Tidal Error of Filters

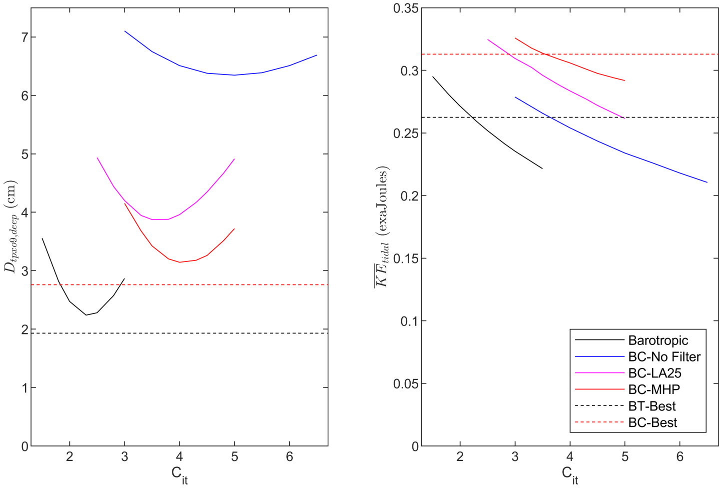

# Tidal Results of ADCIRC2D$^+$

- The improvement in results when internal wave dissipation is applied only at the tidal frequencies provides strong evidence that internal waves in the deep ocean are generated at tidal frequencies.
- Due to the extreme sensitivity of global tides to changes in barotropic to baroclinic conversion, filtering is necessary when parameterizing internal tide dissipation.
- It is not simply a matter of matching the tidal kinetic energy in a system to ensure accurate tidal results.

# Tidal Results of ADCIRC2D$^+$

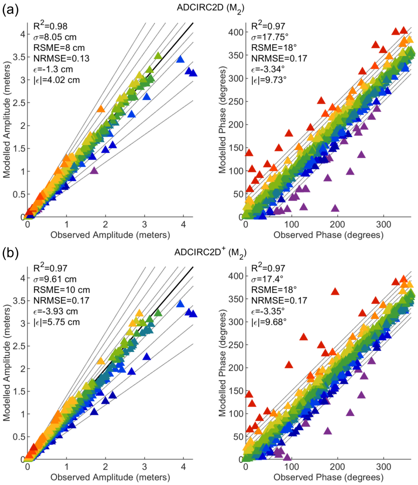

# Tidal Results of ADCIRC2D$^+$

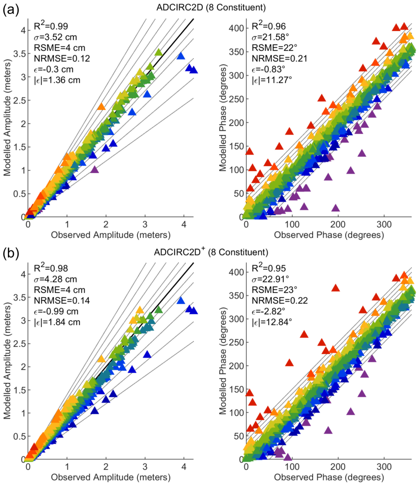

# Tidal Results of ADCIRC2D$^{+}$

| Error Metric | ADCIRC2D | ADCIRC2D$^{+}$ |
|---|---|---|
| $D_{M_2,stations}$ (cm) | 6.81 | 7.77 |
| $D_{M_2,tpxo9,deep}$ (cm) | 1.94 | 2.76 |
| $D_{M_2,tpxo,shallow}$ (cm) | 7.87 | 10.13 |

# Non-Tidal Results of ADCIRC2D$^+$

Measures of Model Skill:

$$\gamma^2 = \frac{Var(\eta_m - \eta_o)}{Var(\eta_o)}$$

$$Skill = 1 - \frac{\int_0^T (\eta_m - \eta_o)^2 dt}{\int_0^T (|\eta_m - \overline{\eta}_o| + |\eta_o - \overline{\eta}_o|)^2 dt}$$

$$RMSE = \left[\frac{1}{T}\int_0^T (\eta_m - \eta_o)^2 dt\right]^{\frac{1}{2}}$$

# Non-Tidal Results of ADCIRC2D$^+$

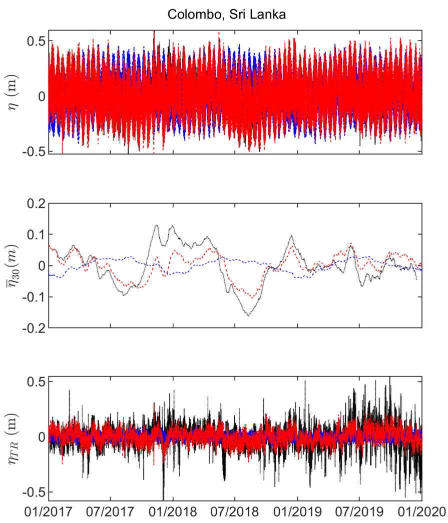

# Non-Tidal Results of ADCIRC2D$^{+}$

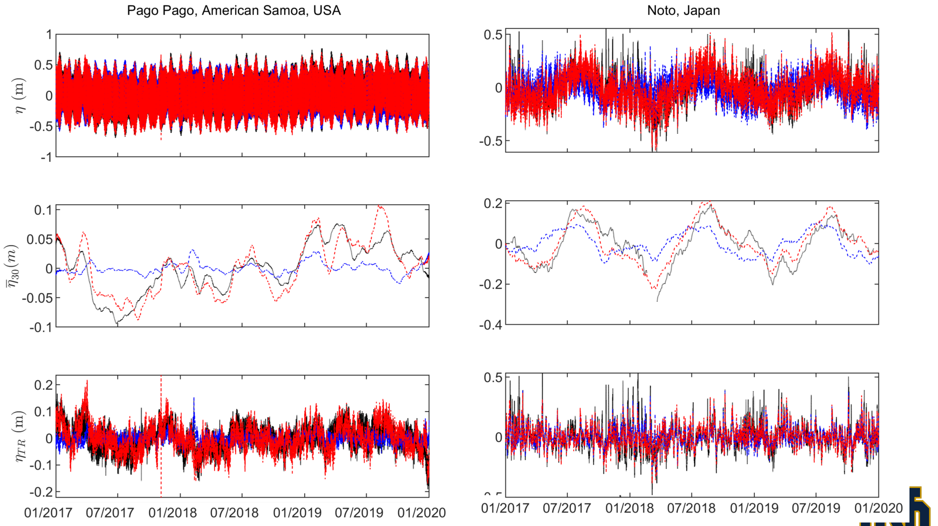

# Non-Tidal Results of ADCIRC2D$^{+}$

| Measure | Pago Pago, USA | Colombo, SRL | Noto, JPN | Atka, USA | Mean |
|---|---|---|---|---|---|
| $\gamma^2_{TWL,BT}$ | 0.04 | 1.10 | 0.58 | 0.05 | 0.44 |
| $\gamma^2_{TWL,BC}$ | 0.04 | 0.86 | 0.30 | 0.08 | 0.40 |
| $Skill_{TWL,BT}$ | 0.99 | 0.76 | 0.79 | 0.99 | 0.90 |
| $Skill_{TWL,BC}$ | 0.99 | 0.82 | 0.92 | 0.98 | 0.91 |
| $RMSE_{TWL,BT}(cm)$ | 5.60 | 14.80 | 11.90 | 8.20 | 28.58 |
| $RMSE_{TWL,BC}(cm)$ | 6.00 | 13.10 | 8.60 | 10.60 | 27.95 |
| $\gamma^2_{\overline{\eta}_{30},BT}$ | 0.93 | 1.39 | 0.89 | 0.14 | 0.70 |
| $\gamma^2_{\overline{\eta}_{30},BC}$ | 0.30 | 0.43 | 0.22 | 0.07 | 0.40 |
| $Skill_{\overline{\eta}_{30},BT}$ | 0.30 | 0.07 | 0.59 | 0.96 | 0.57 |
| $Skill_{\overline{\eta}_{30},BC}$ | 0.93 | 0.82 | 0.94 | 0.98 | 0.81 |
| $RMSE_{\overline{\eta}_{30},BT}$ (cm) | 4.00 | 7.20 | 8.90 | 2.60 | 7.92 |
| $RMSE_{\overline{\eta}_{30},BC}$ (cm) | 2.20 | 4.00 | 4.40 | 1.90 | 6.13 |
| $\gamma^2_{\eta_{NTR},BT}$ | 0.93 | 1.01 | 0.42 | 0.08 | 0.65 |
| $\gamma^2_{\eta_{NTR},BC}$ | 1.07 | 0.99 | 0.41 | 0.14 | 0.79 |
| $Skill_{\eta_{NTR},BT}$ | 0.49 | 0.25 | 0.84 | 0.98 | 0.61 |
| $Skill_{\eta_{NTR},BC}$ | 0.75 | 0.53 | 0.86 | 0.97 | 0.66 |
| $RMSE_{\eta_{NTR},BT}$ (cm) | 3.80 | 9.90 | 7.30 | 3.60 | 17.70 |
| $RMSE_{\eta_{NTR},BC}$ (cm) | 4.10 | 9.80 | 7.20 | 4.80 | 18.52 |

- Total water level errors stayed largely the same

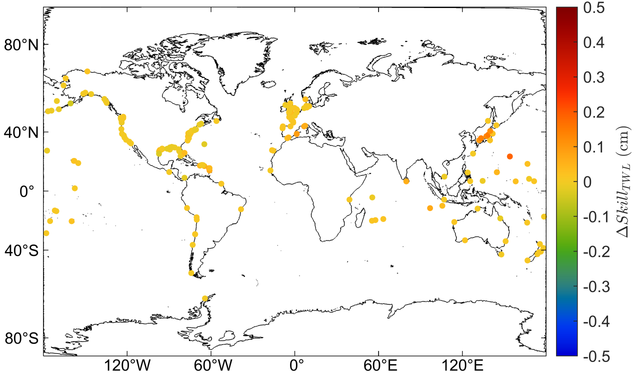

# Non-Tidal Results of ADCIRC2D$^{+}$ (Highlights)

- Total water level errors stayed largely the same
- Non tidal residual errors saw modest improvement mid-latitudes but on average stayed the same

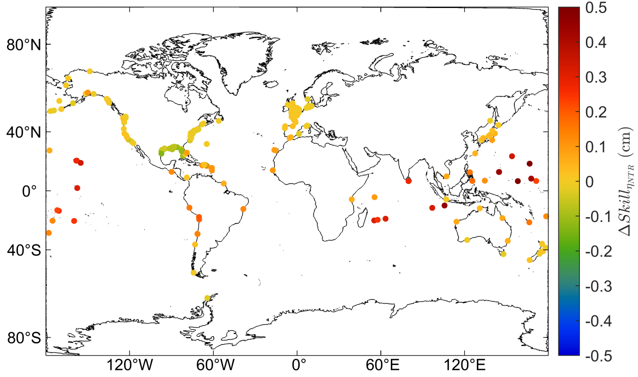

- Total water level errors stayed largely the same
- Non tidal residual errors saw modest improvement mid-latitudes but on average stayed the same
- 30-day average sea levels saw drastic improvement at mid-latitudes and modest

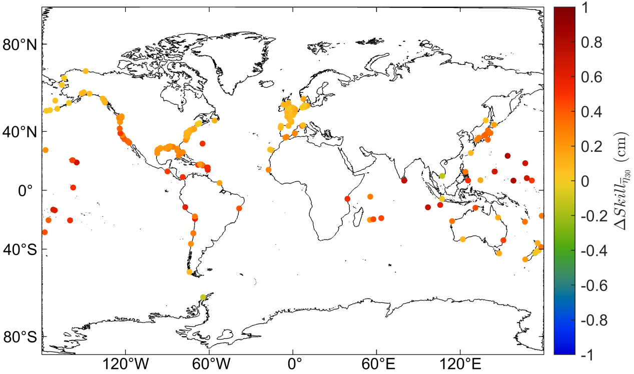

# Conclusions

- Sensitivity to internal tide dissipation (and other dissipative parameters) is highlighted. Without accurate (both temporally and spatially) capture of this phenomenon, global tides will not be accurately captured.
- Inclusion of density-driven effects—even in depth-averaged form—can greatly improve mean sea level predictions of a high-resolution total water level model.
- Further evidence that deep-water internal waves (and their ensuing dissipation) are generated predominantly at tidal frequencies.

# Overview

# Summary

- It is possible to downscale coarse OGCM data to the scale of high-resolution, depth-averaged total water level models and capture density-driven effects without the high overhead of solving the full 3D equations on the high-resolution mesh.

# Summary

- It is possible to downscale coarse OGCM data to the scale of high-resolution, depth-averaged total water level models and capture density-driven effects without the high overhead of solving the full 3D equations on the high-resolution mesh.
- Filtering out low-frequency energy in the velocity signal for the internal tide dissipation parameter helps to spatially and temporally apply this phenomena to the correct areas, helping to improve tidal results in baroclinic models.

# Summary

- It is possible to downscale coarse OGCM data to the scale of high-resolution, depth-averaged total water level models and capture density-driven effects without the high overhead of solving the full 3D equations on the high-resolution mesh.
- Filtering out low-frequency energy in the velocity signal for the internal tide dissipation parameter helps to spatially and temporally apply this phenomena to the correct areas, helping to improve tidal results in baroclinic models.
- The fact that the tidal signal is improved with higher quality filtering provides further evidence that internal waves are generated in the deep ocean at tidal frequencies.

# Future Work

- Apply ADCIRC2D$^{+}$ to the ND-CHL/NOAA Global Storm Tide Operational Forecasting System (GSTOFS).
  - High resolution (80 m to 25 km) unstructured global model.
  - This work includes performing 12-year hindcasts on this high-resolution model.

# Future Work

- Apply ADCIRC2D$^{+}$ to the ND-CHL/NOAA Global Storm Tide Operational Forecasting System (GSTOFS).
  - High resolution (80 m to 25 km) unstructured global model.
  - This work includes performing 12-year hindcasts on this high-resolution model.
- Work with other members of ND-CHL to couple ADCIRC not only to GOFS3.1 but also to the National Water Model (NWM).

# Future Work

- Apply ADCIRC2D$^+$ to the ND-CHL/NOAA Global Storm Tide Operational Forecasting System (GSTOFS).
  - High resolution (80 m to 25 km) unstructured global model.
  - This work includes performing 12-year hindcasts on this high-resolution model.
- Work with other members of ND-CHL to couple ADCIRC not only to GOFS3.1 but also to the National Water Model (NWM).
- Use more refined parameter estimation techniques (EnKF, etc.) to find optimal friction coefficients.

# Future Work

- Apply ADCIRC2D$^{+}$ to the ND-CHL/NOAA Global Storm Tide Operational Forecasting System (GSTOFS).
  - High resolution (80 m to 25 km) unstructured global model.
  - This work includes performing 12-year hindcasts on this high-resolution model.
- Work with other members of ND-CHL to couple ADCIRC not only to GOFS3.1 but also to the National Water Model (NWM).
- Use more refined parameter estimation techniques (EnKF, etc.) to find optimal friction coefficients.
- Examine (even) more refined filters and their frequency responses in the coupled model.
  - This could include using high-pass filters on supertidal energy in coastal zones where internal waves are generated at higher frequency!
  - Could apply separate filters to diurnal and semidiurnal frequencies to see the impacts of different frequencies on tidal amplitudes.

# Acknowledgements


Special thanks to:

- Dr. Joannes Westerink
- Dr. Joe Fernando, Dr. Al Cerrone, and Dr. Andrew Kennedy
- Dr. Damrongsak Wirasaet
- Dr. Guoming Ling
- María Teresa Contreras
- Dr. William Pringle
- Collaborators at NOAA and the Army Corp of Engineers
- National Science Foundation PREEVENTS, NOAA JTTI
- All of you!

# Thank you

Questions?

# References I


[1] Brian K Arbic. Incorporating tides and internal gravity waves within global ocean general circulation models: A review. *Progress in Oceanography*, 206:102824, 2022.

[2] John Atkinson, Hugh Roberts, Scott Hagen, Shan Zou, Peter Bacopoulos, Stephen Medeiros, John Weishampel, and Zachary Cobell. Deriving Frictional Parameters and Performing Historical Validation for an ADCIRC Storm Surge Model of the Florida Gulf Coast. *Florida Watershed Journal*, 4, 1 2011.

[3] Coleman P. Blakely, Guoming Ling, William J. Pringle, María Teresa Contreras, Damrongsak Wirasaet, Joannes J. Westerink, Saeed Moghimi, Greg Seroka, Lei Shi, Edward Myers, Margaret Owensby, and Chris Massey. Dissipation and Bathymetric Sensitivities in an Unstructured Mesh Global Tidal Model. *Journal of Geophysical Research: Oceans*, 127(5):e2021JC018178, 5 2022.

# References II


[4] James A Cummings. Operational multivariate ocean data assimilation. *Quarterly Journal of the Royal Meteorological Society*, 131(613):3583–3604, 10 2005.

[5] G D Egbert and R D Ray. Significant dissipation of tidal energy in the deep ocean inferred from satellite altimeter data. *Nature*, 405(6788):775–778, 2000.

[6] Hongli Fu, Xinrong Wu, Wei Li, Lianxin Zhang, Kexiu Liu, and Bo Dan. Improving the accuracy of barotropic and internal tides embedded in a high-resolution global ocean circulation model of MITgcm. *Ocean Modelling*, 162:101809, 2021.

[7] Gordon W. Groves. Numerical filters for discrimination against tidal periodicities. *Eos, Transactions American Geophysical Union*, 36(6):1073–1084, 12 1955.

# References III


[8] P C Kerr, R C Martyr, A S Donahue, M E Hope, J J Westerink, R A Luettich Jr., A B Kennedy, J C Dietrich, C Dawson, and H J Westerink. U.S. IOOS coastal and ocean modeling testbed: Evaluation of tide, wave, and hurricane surge response sensitivities to mesh resolution and friction in the Gulf of Mexico. *Journal of Geophysical Research: Oceans*, 118(9):4633–4661, 9 2013.

[9] E Joseph Metzger, R W Helber, Patrick J Hogan, Pamela G Posey, Prasad G Thoppil, L Townsend Tamara, Alan J Wallcraft, Ole Martin Smedstad, Deborah S Franklin, Luis Zamudio-Lopez, and Michael W Phelps. Global Ocean Forecast System 3.1 Validation Testing. Technical report, Naval Research Laboratory, Stennis Space Center, MS 39529-5004, 2017.

[10] NOAA. National coastal population report: Population trends from 1970 to 2020. *NOAA State Coast Rep. Ser.*, 2013.

# References IV

[11] W J Pringle, D Wirasaet, K J Roberts, and J J Westerink. Global storm tide modeling with ADCIRC v55: unstructured mesh design and performance. *Geosci. Model Dev.*, 14(2):1125–1145, 2 2021.

[12] William J. Pringle, Damrongsak Wirasaet, Andika Suhardjo, Jessica Meixner, Joannes J. Westerink, Andrew B. Kennedy, and Shangyao Nong. Finite-Element barotropic model for the Indian and Western Pacific Oceans: Tidal model-data comparisons and sensitivities. *Ocean Modelling*, 129:13–38, 9 2018.

[13] Y J Zhang, T Fernandez-Montblanc, W Pringle, H.-C. Yu, L Cui, and S Moghimi. Global seamless tidal simulation using a 3D unstructured-grid model (SCHISM v5.10.0). *Geoscientific Model Development*, 16(9):2565–2581, 2023.

# Tide results in current hydrodynamic models

Table: Comparisons of tidal results of a selection of hydrodynamic models.

| Model | Resolution | $D_{M_2,deep}$ (cm)[2] | $D_{M_2,shallow}$ (cm)[1] | Source |
|---|---|---|---|---|
| MITgcm[3] | 9 km | 32.33 | - | [6] |
| HYCOM[3] | 12.5 km | 4.4 | - | [1] |
| SCHISM | 2-15 km | 4.2 | 14.3 | [13] |
| ADCIRC2D | 2-25 km | 1.93 | 7.87 | [3] |
| ADCIRC2D$^+$ | 2-25 km | 2.76 | 10.13 | - |

[2]Compared to TPXO9-atlas [5]
[3]Non-data assimilated

# ADCIRC2D$^+$ Error Metrics

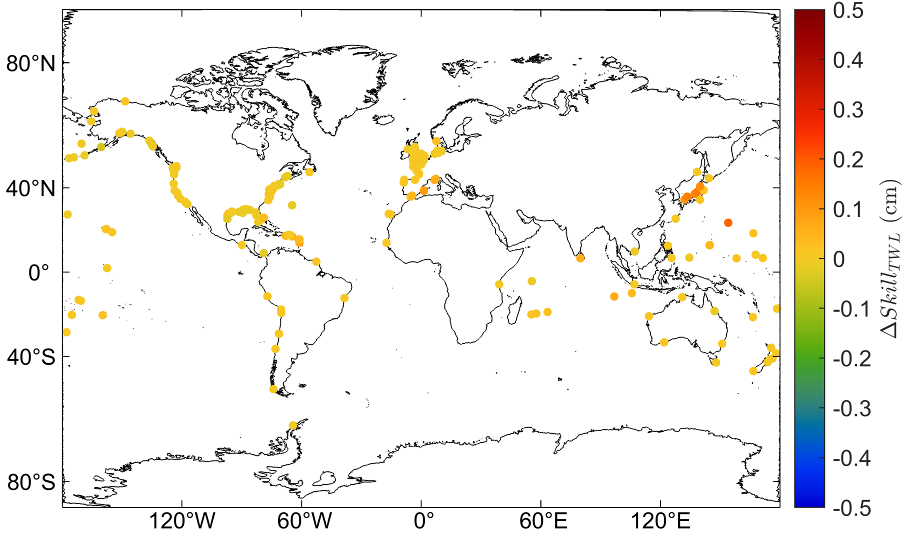

# ADCIRC2D$^+$ Error Metrics

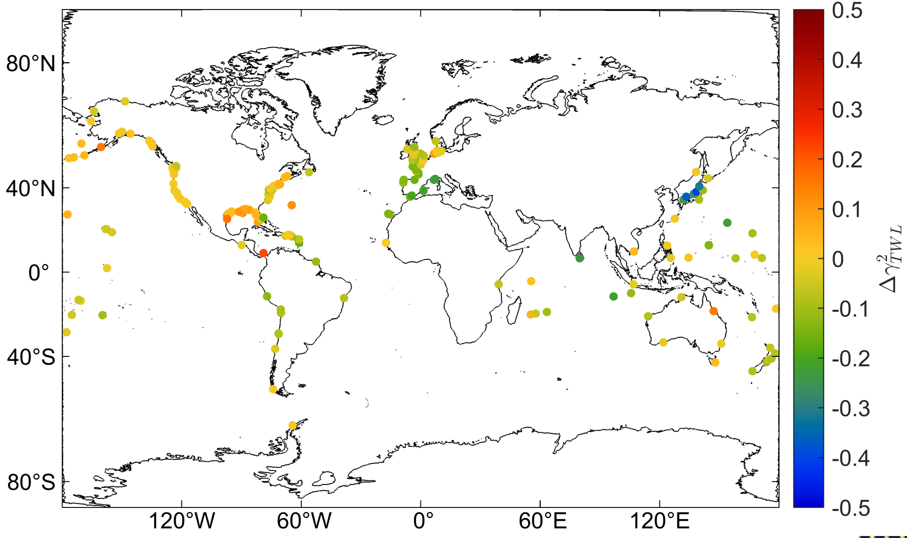

# ADCIRC2D$^+$ Error Metrics

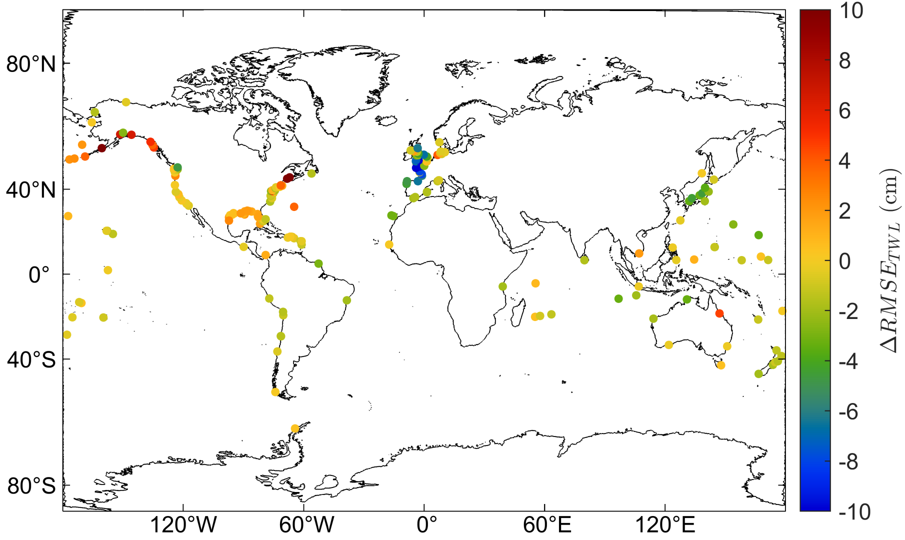

# ADCIRC2D$^+$ Error Metrics

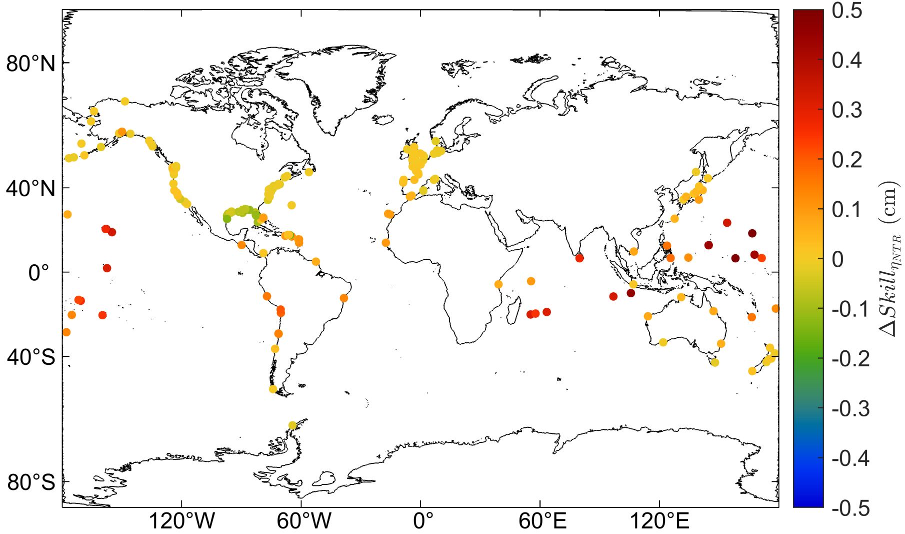

# ADCIRC2D$^{+}$ Error Metrics

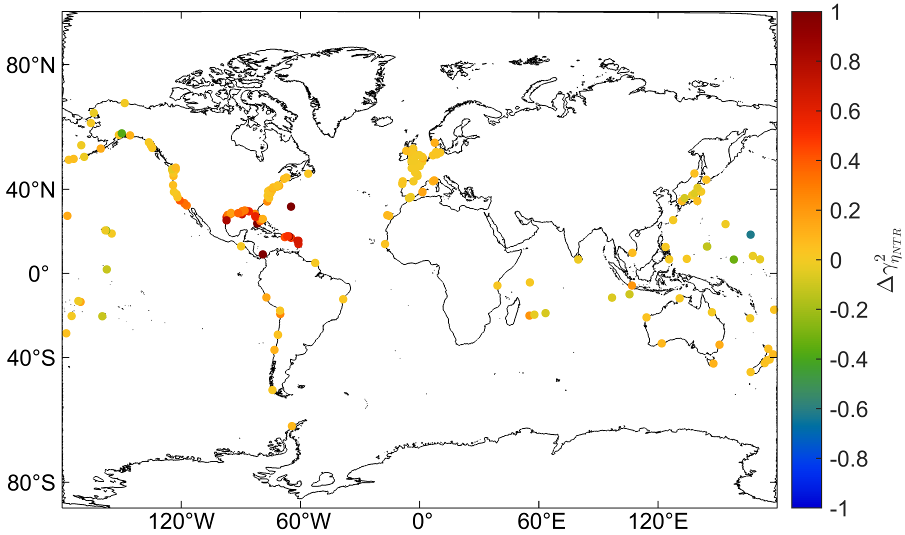

# ADCIRC2D$^+$ Error Metrics

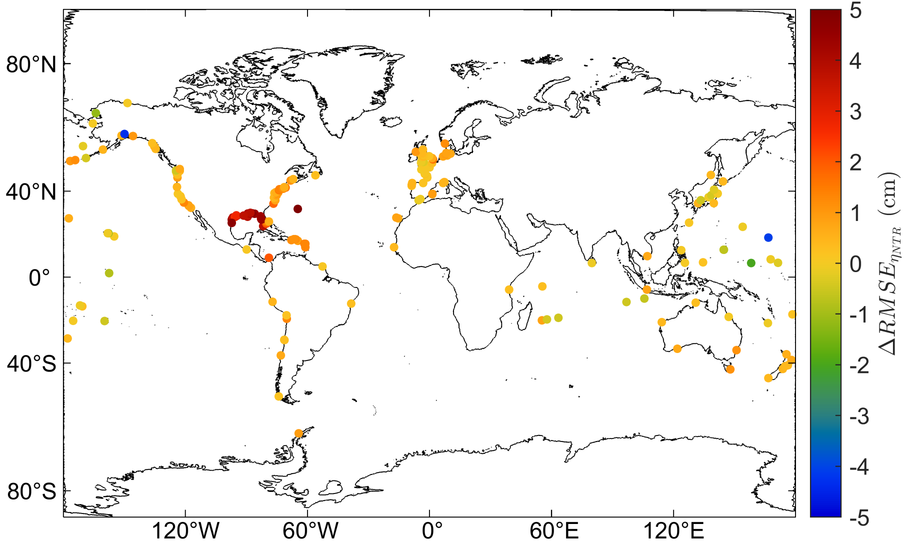

# ADCIRC2D$^+$ Error Metrics

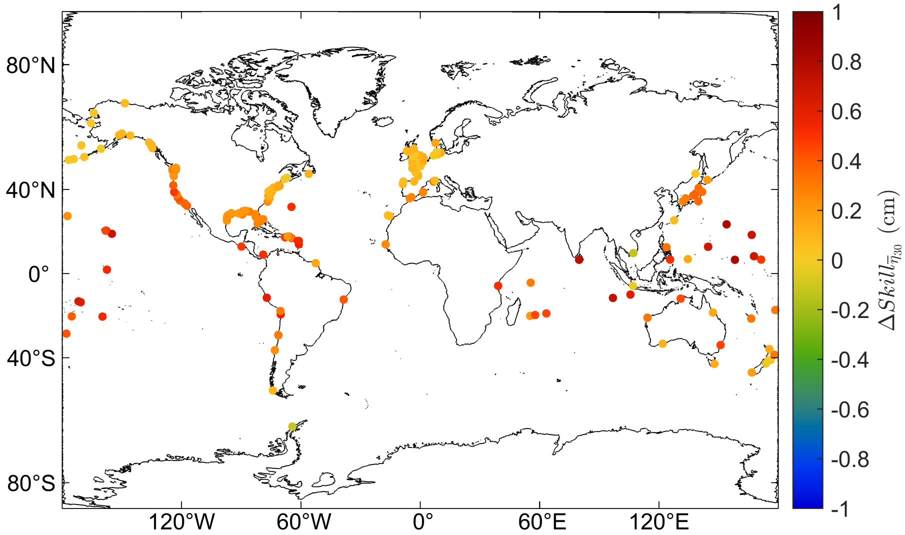

# ADCIRC2D$^+$ Error Metrics

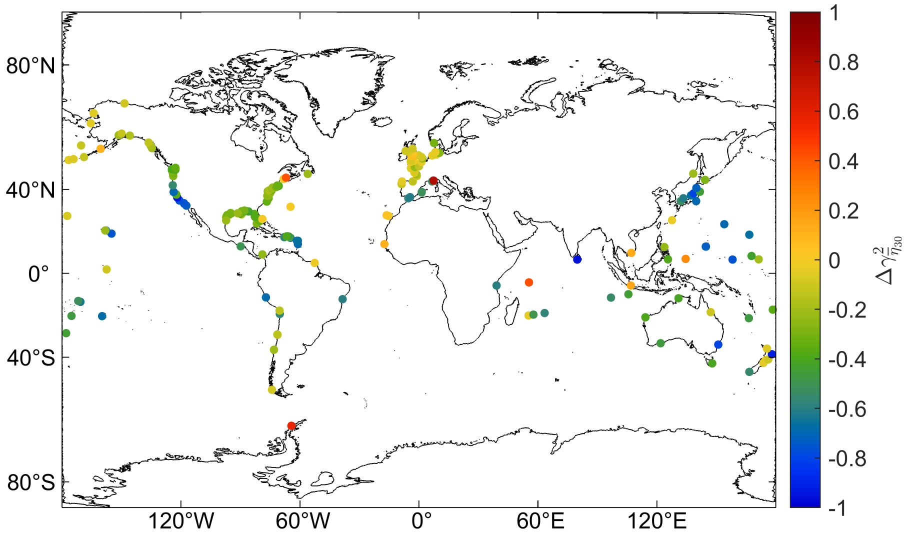

# ADCIRC2D$^+$ Error Metrics

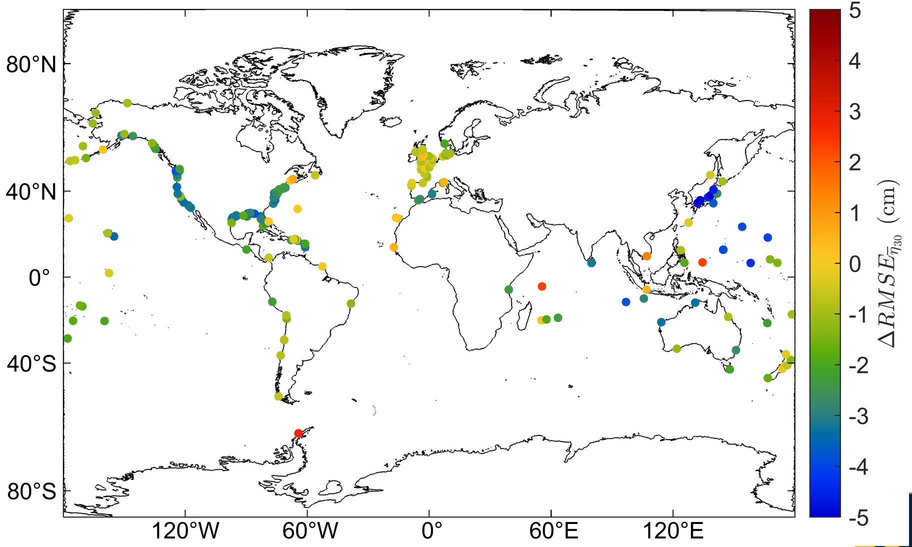

# Baroclinic Internal Tide Tensor

$$\nabla h \cdot \boldsymbol{U_T} \nabla h = \begin{bmatrix} h_x^2 & h_x h_y \\ h_x h_y & h_y^2 \end{bmatrix} \cdot \boldsymbol{A} \cdot \boldsymbol{U}$$

$$\boldsymbol{A} = \frac{1}{2}\boldsymbol{A}^* + \boldsymbol{A}^{\boldsymbol{T}*} = \begin{bmatrix} \frac{u_T}{u} & \frac{1}{2}(\frac{u_T}{u} + \frac{v_T}{v}) \\ \frac{1}{2}(\frac{u_T}{u} + \frac{v_T}{v}) & \frac{v_T}{v} \end{bmatrix}$$

$$\boldsymbol{A}^* = \begin{bmatrix} \frac{u_T}{u} & \frac{v_T}{v} \\ \frac{u_T}{u} & \frac{v_T}{v} \end{bmatrix}$$

# Mesh-Dependency of $C_{it}$

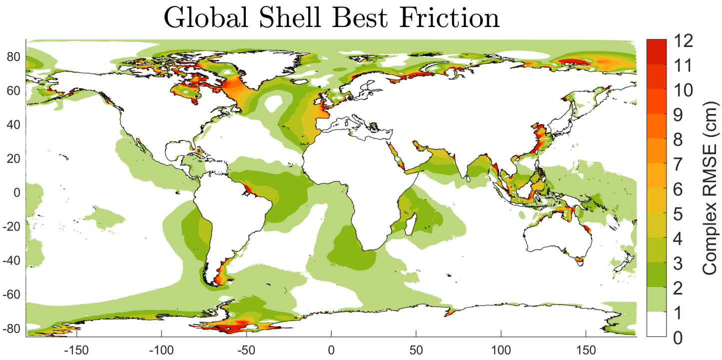


- $C_{it}$ is highly mesh-dependent
- When optimal $C_{it}$ from RG1 is applied to high-resolution forecasting mesh, results degrade

# Mesh-Dependency of $C_{it}$

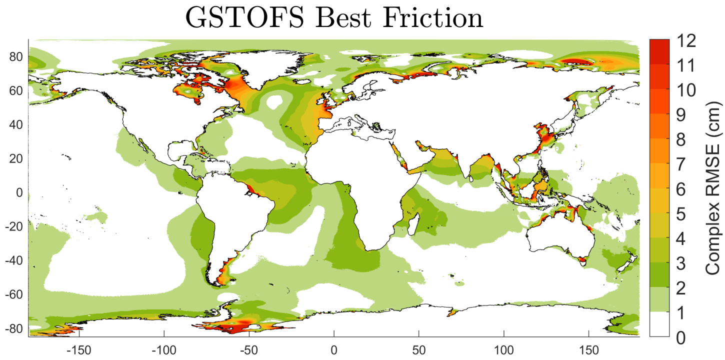


- $C_{it}$ is highly mesh-dependent
- When optimal $C_{it}$ from RG1 is applied to high-resolution forecasting mesh, results degrade

# Cost Function

$$Z^k_{o,m} = Re^k_{o,m} + iIm^k_{o,m}$$
$$Z^k_{b,m} = Re^k_{b,m} + iIm^k_{b,m}$$
$$f^k_m(\boldsymbol{x}) = g^k_m(\boldsymbol{x}) + ih^k_m(\boldsymbol{x})$$
$$g^k_m(\boldsymbol{x}) = \sum_{j=1}^{M} g^k_{j,m}(x_j)$$
$$h^k_m(\boldsymbol{x}) = \sum_{j=1}^{M} h^k_{j,m}(x_j)$$
$$Z^k_{m,i} = Z^k_{b,i} + f^k_i(\boldsymbol{x})$$

# Approach 1: External Forcing

$$u(t) = \sum_{i=1}^{N} f_i U_i cos(a_i t + \{V_o + u\}_i - \kappa_i)$$

$$v(t) = \sum_{i=1}^{N} f_i V_i cos(a_i t + \{V_o + u\}_i - \kappa_i)$$

$\langle u, v \rangle$ = Meridional and zonal tidal velocities

$f_i$ = Nodal factor of $i^{th}$ tidal constituent[4]

$\langle U_i, V_i \rangle$ = Amplitudes of tidal velocities

$a_i$ = Frequency of $i^{th}$ tidal constituent

$\{V_o + u\}_i$ = Equilibrium argument of $i^{th}$ tidal constituent

$\kappa_i$ = Phase lag of $i^{th}$ tidal constituent

[4] Used 8 major constituents: $M_2$, $Q_1$, $O_1$, $P_1$, $K_1$, $N_2$, $S_2$, and $K_2$

# Approach 1: External Forcing

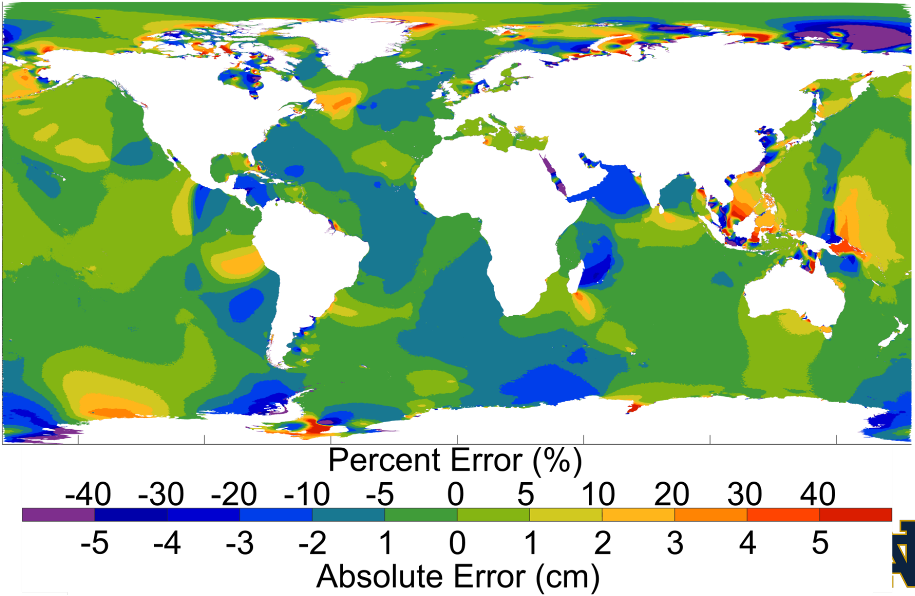

# Approach 1: External Forcing

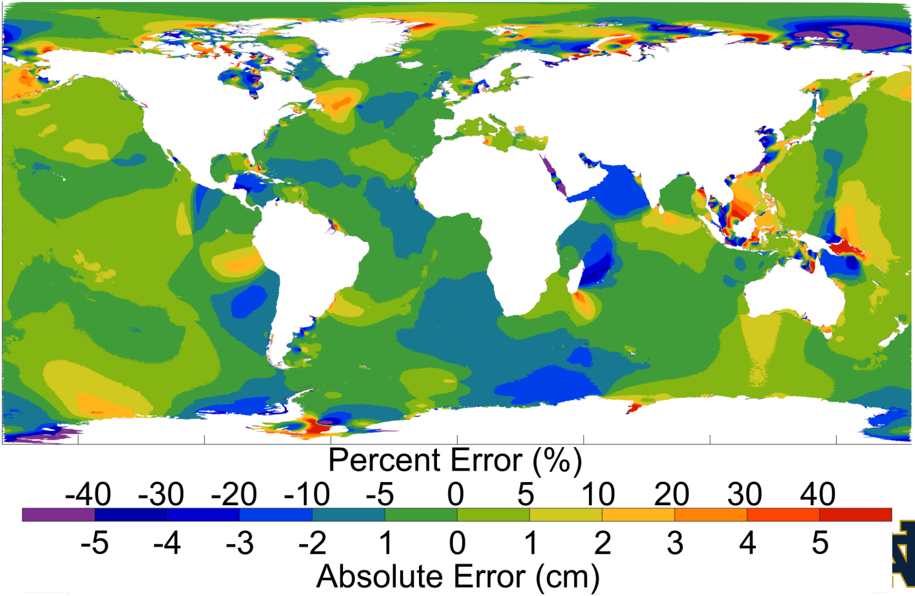

# Approach 1: External Forcing

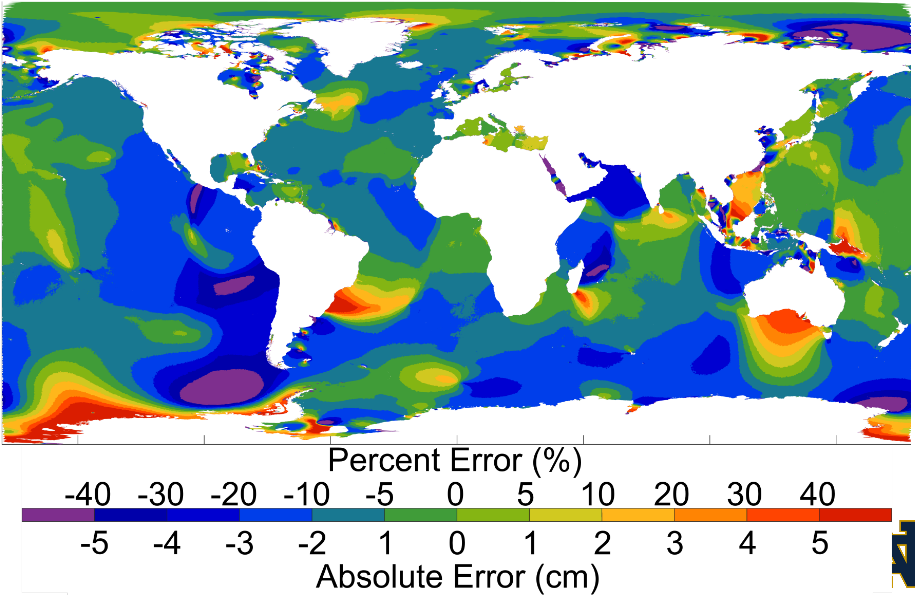

# Approach 1: External Forcing

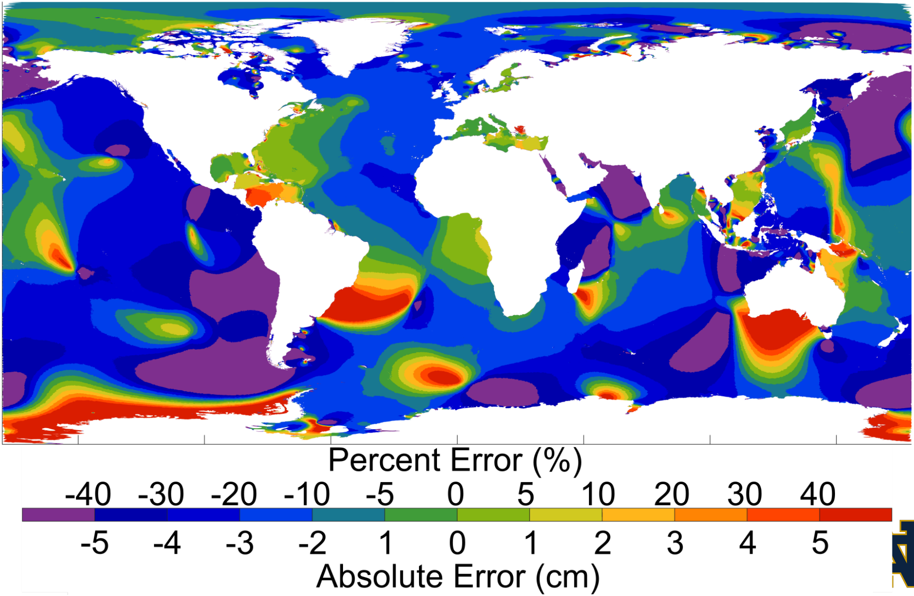

# Approach 1: External Forcing

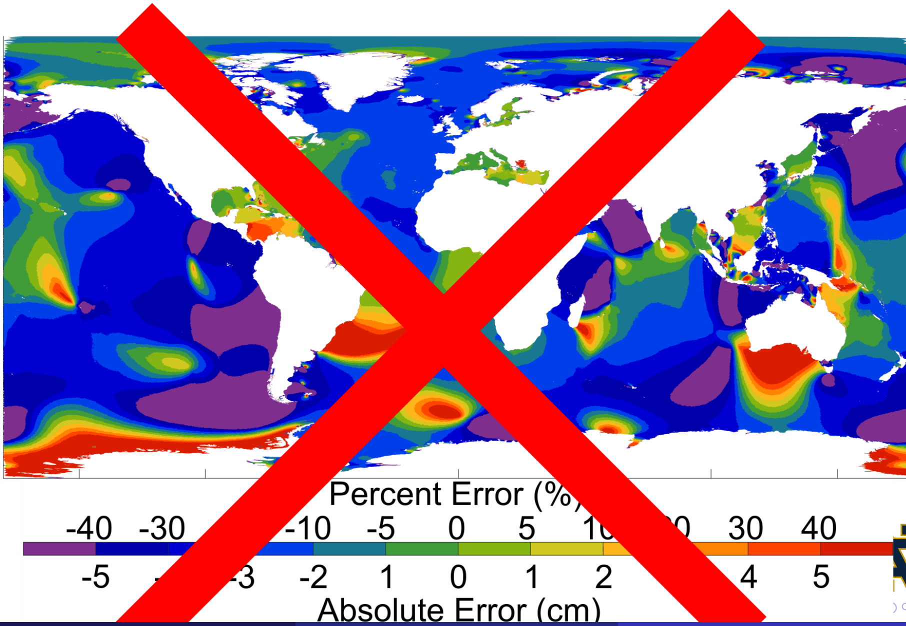

## Lessons Learned

- While it is possible to use external estimates for forcing terms (i.e., $\eta_{SAL}$, $BPG$, etc.), external extimates of dissipation do not appear to work.
- Without an in-line calculation of dissipation parameter, the system is not able to react to changes in dissipation.
- As will be shown, exactly matching the tidal dissipation is not adequate to avoid degradation of tidal results.

# Downscaling of GOFS3.1 Salinity and Temperature Data

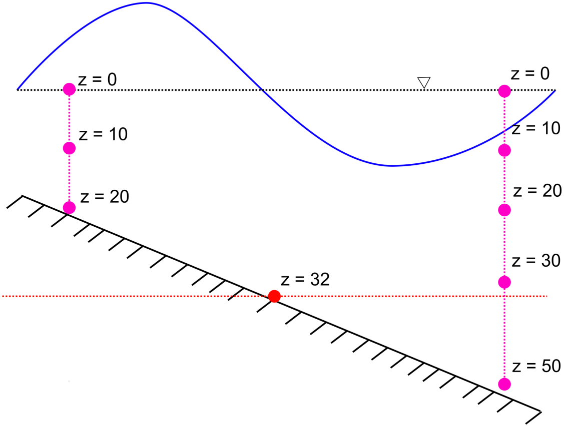

# Downscaling of GOFS3.1 Salinity and Temperature Data

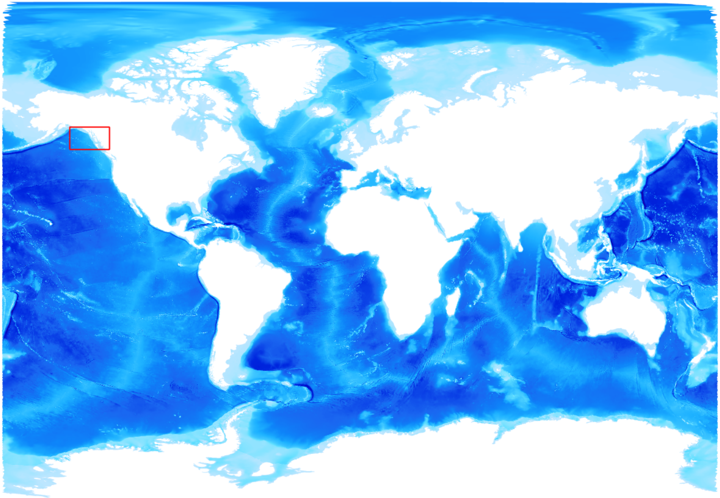

# Downscaling of GOFS3.1 Salinity and Temperature Data

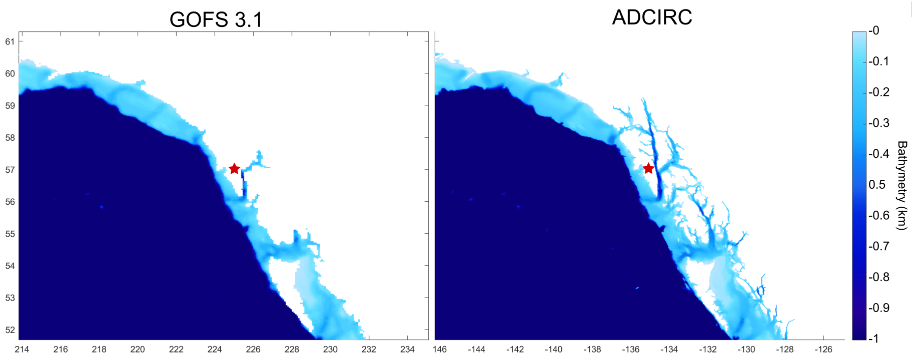

# Downscaling of GOFS3.1 Salinity and Temperature Data

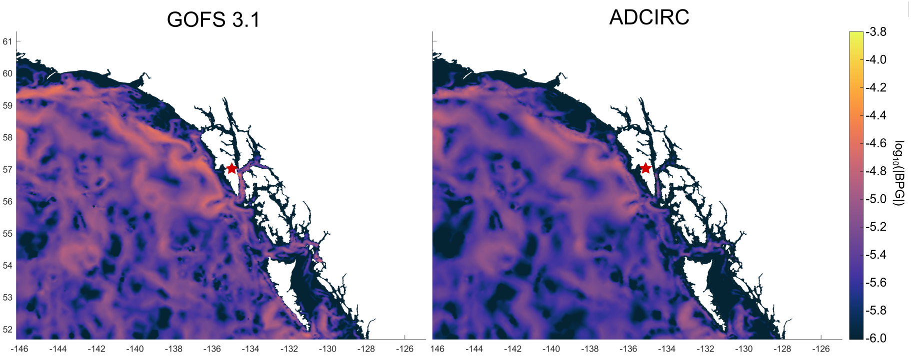

# Non-Tidal Results of ADCIRC2D$^{+}$

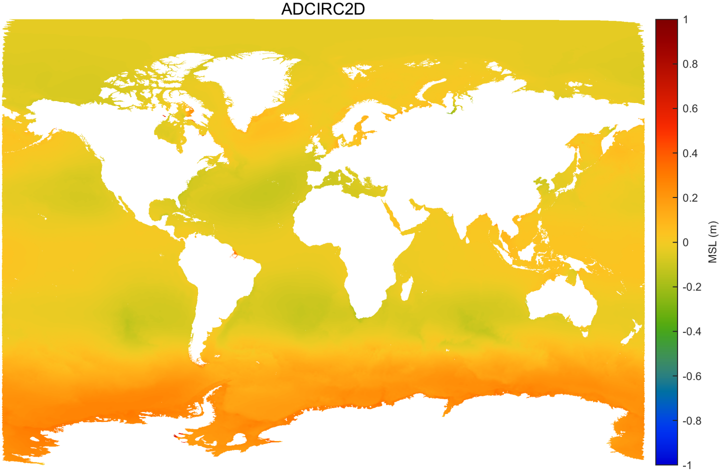

# Non-Tidal Results of ADCIRC2D$^+$

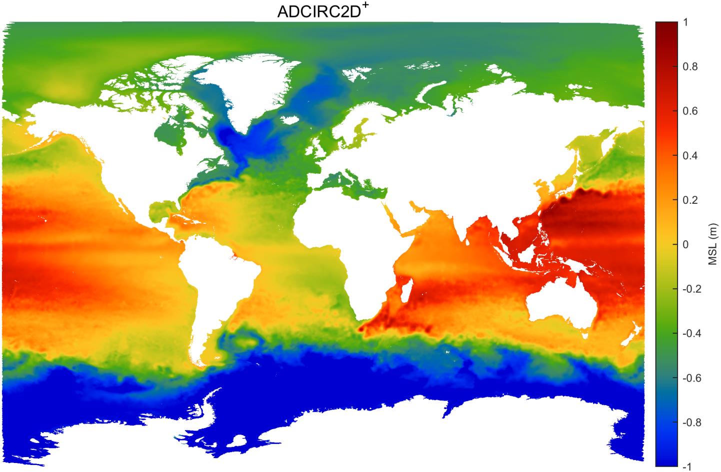

# Non-Tidal Results of ADCIRC2D$^+$

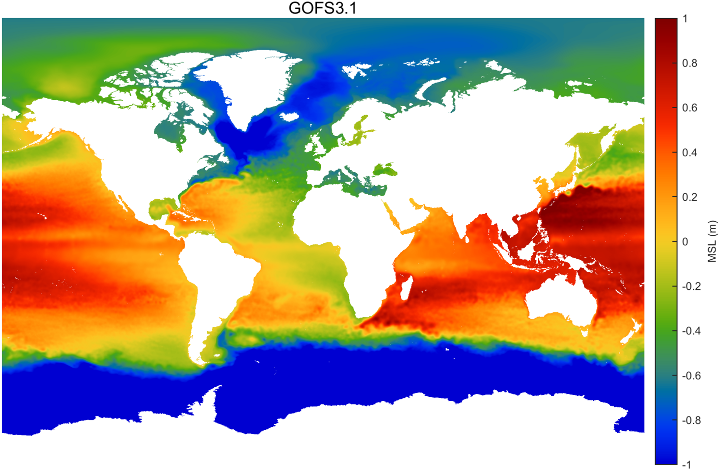

# Non-Tidal Results of ADCIRC2D$^+$

Table: Differences between mean sea levels of ADCIRC models and GOFS3.1 calculated over the time period January 1, 2017 to January 1, 2020.

| Model | $\overline{E}$ (cm) | $\overline{|E|}$ (cm) |
|---|---|---|
| ADCIRC2D | -0.82 | 52.43 |
| ADCIRC2D$^+$ | 0.42 | 14.71 |
| ADCIRD2D Detided | -0.81 | 52.01 |
| ADCIRC2D$^+$ Detided | 0.43 | 13.36 |

# Storm Drawdown